PHYSICAL REVIEW B **78**, 060507(R) (2008)

Superconductivity of Mo_3Sb_7 from first principles

B. Wiendlocha,[1,*] J. Tobola,[1] M. Sternik,[2] S. Kaprzyk,[1] K. Parlinski,[2] and A. M. Oleś[2]
[1]*Faculty of Physics and Applied Computer Science, AGH University of Science and Technology, Al. Mickiewicza 30, PL-30059 Cracow, Poland*
[2]*Institute of Nuclear Physics, Polish Academy of Sciences, Radzikowskiego 152, PL-31342 Cracow, Poland*
(Received 5 June 2008; published 25 August 2008; publisher error corrected 27 August 2008)

Superconductivity in Mo_3Sb_7 is analyzed using the combined electronic structure and phonon calculations, and the *electron-phonon coupling* constant $\lambda_{ph}=0.54$ is determined from first principles. This value explains the experimental value of the superconducting critical temperature $T_c=2.2$ K. The possible influence of spin fluctuations and spin gap on the superconductivity in Mo_3Sb_7 is discussed, and electron-paramagnon interaction is found to be weak.

DOI: 10.1103/PhysRevB.78.060507 PACS number(s): 74.25.Jb, 74.25.Kc, 74.62.Dh

A paramagnetic intermetallic compound Mo_3Sb_7 is a type-II superconductor,[1,2] with the critical temperature $T_c \simeq 2.2$ K. The temperature characteristics of the specific heat, the superconducting gap, and the magnetic critical field suggest that the conventional electron-phonon interaction might be responsible for the superconductivity.[2–5] Recently, however, Candolfi *et al.*[3] argued that spin fluctuations (SFs) are present in Mo_3Sb_7. This interpretation is supported by two unusual features: (i) the quadratic temperature dependence of both electrical resistivity and magnetic susceptibility, as well as (ii) the high value of the susceptibility at room temperature. They also reported a much smaller value of the electronic specific heat jump[3] at the transition point $\Delta C/\gamma T_c = 1.04$ than the weak-coupling BCS value of 1.43, which might suggest additional enhancement of the electronic specific-heat coefficient by the SFs. Very recently, Tran *et al.*[6] observed a peak in the specific heat $C_P(T)$ at $T^*=50$ K, which was interpreted as supporting the presence of spin gap. Also, they explained the anomalous behavior of the magnetization and resistivity in terms of the gap opening. Moreover, they analyzed the electronic specific heat in the superconducting state in terms of the two BCS gap model,[4] and reported a higher value of $\Delta C/\gamma T_c=1.56$ than the one measured before.[3]

In order to elucidate the possible origin of superconductivity, an *ab initio* approach, which involves the electronic structure and phonon calculations, may be used to determine the electron-phonon coupling (EPC) constant. For instance, a recent determination of the EPC constant suggested that the superconductivity in $PuCoGa_5$ is driven by an unconventional mechanism based on antiferromagnetic (AF) fluctuations.[7] Here we present an *ab initio* study of the EPC constant and superconductivity in Mo_3Sb_7, where SFs might play a role. The electron-phonon interaction is treated within the rigid muffin-tin (MT) approximation. The superconducting critical temperature T_c and its possible modification by SFs are discussed using two approaches: (i) the McMillan formula[8,9] and (ii) the equation for T_c, which explicitly includes the presence of paramagnons.[10]

Electronic structure calculations were performed using the Korringa-Kohn-Rostoker (KKR) multiple scattering method.[11] The crystal potential was constructed in the framework of the local density approximation, using von Barth and Hedin formula[12] for the exchange-correlation part. For all atoms angular momentum cutoff $l_{max}=4$ was set; **k**-point mesh in the irreducible part of the Brillouin zone (BZ) contained about 400 points. Density of states (DOS) was computed using the tetrahedron **k**-space integration technique, generating about 1500 tetrahedrons in the irreducible part of the BZ. Semirelativistic calculations results are presented here. Since our main goal in this work is to estimate the EPC constant from first principles within the rigid MT approximation, spherical potential approximation for the crystal potential is used, as is required in this approach. Mo_3Sb_7 crystallizes in a cubic *bcc* structure (space group Im $3m$) of the Ir_3Ge_7 type, with lattice constant[13] $a=9.58$ Å. The primitive cell of Mo_3Sb_7 contains two formula units, i.e., 20 atoms, occupying three nonequivalent positions: Mo in (12e) with $x=0.3432$, Sb(1) in (12d), and Sb(2) in (16f) with $x=0.1624$.

The phonon frequencies were determined within the direct method,[14] which utilizes Hellmann-Feynman forces obtained by performing small atomic displacements of nonequivalent atoms from their equilibrium positions. From them the dynamical matrix is determined and diagonalized to obtain the phonon frequencies at each wave vector. The crystal structure optimization and calculations of the complete set of Hellmann-Feynmann forces were performed using the first-principles VASP package,[15] which makes use of the Perdew, Burke, and Ernzerhof (PBE) functional.[16] The calculations were performed on a $\sqrt{2}\times\sqrt{2}\times 1$ supercell (containing 80 atoms) with periodic boundary conditions. The wave functions were sampled according to Monkhorst-Pack scheme with a **k**-point mesh of (4, 4, 4). After the optimization we obtained the lattice parameter $a=9.6405$ Å and the atomic positions of (0.3421, 0, 0), (0.25, 0, 0.5), and (0.1608, 0.1608, 0.1608) for Mo, Sb(1), and Sb(2), respectively. The determined values are in very good agreement with the experimental data.[13]

The electronic structure was computed for the experimental lattice parameters and atomic positions. Total and site-decomposed electronic DOSs of Mo_3Sb_7 are presented in Fig. 1. The most intriguing feature of the electronic spectrum is the presence of a narrow band gap just above the Fermi level, with E_F located in the range of sharply decreasing DOS.[17] In the inset in Fig. 1 one observes that E_F coincides with a local DOS maximum. By analyzing the angular con-

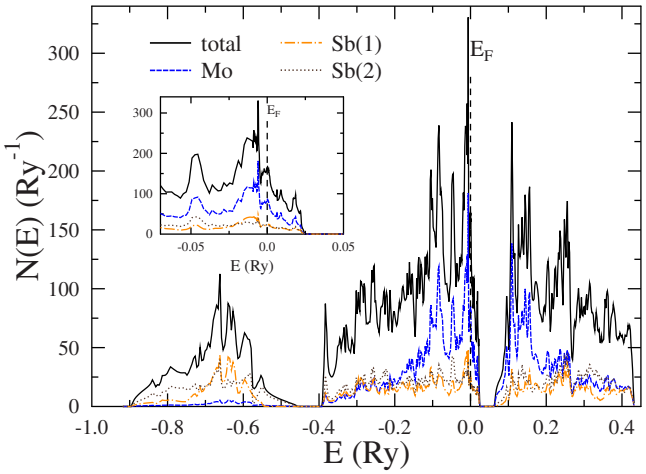

FIG. 1. (Color online) Total and site-decomposed densities of electronic states in Mo_3Sb_7 (per formula unit). The inset shows the details of the DOS near E_F=0.

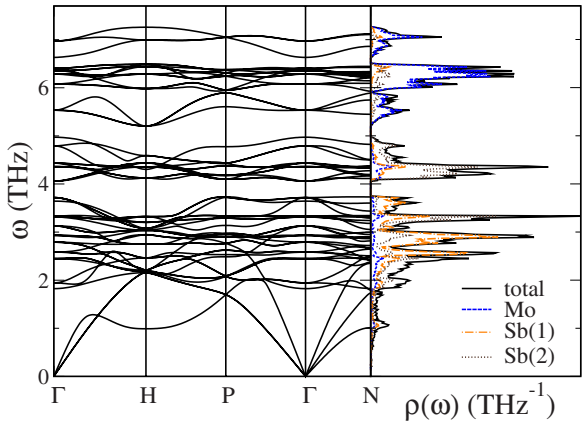

FIG. 2. (Color online) Phonon dispersions along the high-symmetry directions of the BZ (left) and total and site-decomposed densities of phonon states in Mo_3Sb_7 (right). The special points are $\Gamma=(0,0,0)$, $H=(1/2,-1/2,1/2)$, $P=(3/4,-1/4,3/4)$, $\Gamma=(1,0,1)$, and $N=(1,0,1/2)$.

tributions to the total DOS at E_F, presented in Table I, we deduced that the bands near E_F are built out of the Mo($4d$) and Sb($5p$) states. The largest atomic contribution comes from Mo atom, with the value $n_{\mathrm{Mo}}(E_F) \simeq 14$ Ry^{-1}/spin, being not far but below the magnetic instability [the computed Stoner parameter I satisfies $\mathrm{In}_{\mathrm{Mo}}(E_F) \simeq 0.7$]. Note that the spin-polarized KKR calculations assuming ferromagnetic (FM) spin order led to the nonmagnetic ground state.

Tran *et al.*[6] suggested the opening of the spin gap below 50 K, caused by the AF interactions between the selected nearest pairs of Mo atoms. They argued that these atoms form dimers, and the AF interaction stabilizes there spin singlets (but long-range order is absent). We examined a few possible AF structures for this compound, e.g., with alternating moments in Mo planes, but stable AF configuration could not be reached and all magnetic moments converged to zero values. Note, that the proposed model,[6] including one AF and two FM types of Mo-Mo interactions, creates a geometrical frustration of the Mo sublattice. The high value of the DOS at E_F, as well as the suggested different magnetic interactions between Mo atoms, may also give rise to the SFs, which could appear in real sample.

The electronic structure results were used to calculate the electronic part of the EPC constant, i.e., the McMillan-Hopfield η_i parameters[8,18] for each atom. They follow from the formula[19,20]

$$\eta_i = \sum_l \frac{(2l+2)n_l n_{l+1}}{(2l+1)(2l+3)N(E_F)} \left| \int_0^{R_{\mathrm{MT}}} r^2 R_l \frac{\mathrm{dV}}{\mathrm{dr}} R_{l+1} \right|^2, \quad (1)$$

where $V(r)$ is the self-consistent potential at site i, R_{MT} is the radius of the i-th MT sphere, $R_l(r)$ is a regular solution of the radial Schrödinger equation (normalized to unity inside the MT sphere), $n_l(E_F)$ is the l-th partial DOS per spin at the Fermi level E_F, and $N(E_F)$ is the total DOS per cell and spin. The values of η_i parameters in Eq. (1), with contributions from each $l \rightarrow l+1$ scattering channels, are presented in Table I. For Mo, the d-f channel is the most important one (typically for d element), whereas p-d contribution dominates for both Sb atoms. The Sb(1) and Sb(2) atoms have very similar η_i parameters, despite quite different p-DOSs. This is a result of opposite behavior in both partial DOSs, i.e., for the Sb(2) atom the lower p-DOS is compensated by the larger value of d-DOS [the radial wave functions matrix elements form Eq. (1) are similar in both cases].

The phonon dispersion relations along the high-symmetry directions and the total and site-decomposed partial phonon DOSs were computed by random sampling of the BZ and are presented in Fig. 2 for the optimized supercell. The optic phonons give three characteristic maxima of the phonon DOS $\rho(\omega)$ at $\omega \simeq 2.8$, 4.4, and 6.3 THz. The Mo atoms, which are about 30% lighter than Sb atoms, contribute mainly to the high-frequency part of the phonon DOS. The phonon DOS was used to compute the average square site-decomposed phonon frequencies $\langle \omega_i^2 \rangle$ presented as well in Table I. These quantities, together with $\{\eta_i\}$ parameters, are needed to deduce the EPC constant

$$\lambda_{\mathrm{ph}} = \sum_i \frac{\eta_i}{M_i \langle \omega_i^2 \rangle} = \sum_i \lambda_i. \quad (2)$$

Here i runs over all the atoms in the primitive cell and M_i is the atomic mass. For a review, more detailed discussion of

TABLE I. Site-decomposed electronic and dynamic properties of Mo_3Sb_7. $n_i(E_F)$ is in Ry^{-1}/spin, η_i in mRy/a_B^2 (both per atom), ω_i in THz. Values of λ_i take into account the number of i-type atoms in the primitive cell: 6 Mo, 6 Sb(1), 8 Sb(2).

Atom	$n_i(E_F)$	$n_s(E_F)$	$n_p(E_F)$	$n_d(E_F)$	$n_f(E_F)$	η_i	η_{sp}	η_{pd}	η_{df}	$\sqrt{\langle \omega_i^2 \rangle}$	λ_i
Mo	14.3	0.05	0.54	13.7	0.04	6.75	0.0	1.3	5.4	5.07	0.19
Sb(1)	3.7	0.09	3.16	0.37	0.06	2.64	0.0	2.6	0.0	2.97	0.17
Sb(2)	3.0	0.13	2.19	0.51	0.17	2.60	0.0	2.6	0.0	3.41	0.17

the approximations involved in this approach, and a number of references to the previous rigid MT studies, is seen in, e.g., Ref. 21 and references therein.

Surprisingly, one finds that all the atoms are equally important for the onset of superconductivity in Mo_3Sb_7. The contribution from Mo atoms to the total λ_{ph}, despite the dominant character of Mo states near E_F, is only slightly larger than those from Sb(1) and Sb(2), respectively. This is a consequence of higher partial phonon frequencies for Mo. It is worth noting that Sb(1) and Sb(2) have the same λ_i values in spite of rather different average phonon frequencies. Here, the effect of higher $\langle\omega_i^2\rangle$ for Sb(2) is compensated by the larger multiplicity of this crystallographic site. The calculated total EPC constant [Eq. (2)] is $\lambda_{ph}=0.54$, which qualifies Mo_3Sb_7 as the medium-coupling superconductor.

We estimated the superconducting critical temperature T_c using two formulas: (i) a McMillan-type formula,[8,9] with the logarithmically averaged phonon frequency $\omega_{ph}\equiv\langle\omega_{log}\rangle$ in the prefactor,

$$T_c=\frac{\omega_{ph}}{1.20}\exp\left\{-\frac{1.04(1+\lambda_{eff})}{\lambda_{eff}-\mu^\star_{eff}(1+0.62\lambda_{eff})}\right\}, \quad (3)$$

and (ii) the formula including the interaction of electrons with paramagnons, and successfully applied before to $MgCNi_3$,[10]

$$T_c=1.14\omega_{ph}^{\lambda_{ph}/(\lambda_{ph}-\lambda_{sf})}\omega_{sf}^{-\lambda_{sf}/(\lambda_{ph}-\lambda_{sf})}e^K \times\exp\left\{-\frac{1+\lambda_{ph}+\lambda_{sf}}{\lambda_{ph}-\lambda_{sf}-\mu^\star\left(1-K\frac{\lambda_{ph}-\lambda_{sf}}{1+\lambda_{ph}+\lambda_{sf}}\right)}\right\}, \quad (4)$$

$$K=-\frac{1}{2}-\frac{\lambda_{ph}\lambda_{sf}}{(\lambda_{ph}-\lambda_{sf})^2}\left[1+\frac{\omega_{ph}^2+\omega_{sf}^2}{\omega_{ph}^2-\omega_{sf}^2}\ln\frac{\omega_{sf}}{\omega_{ph}}\right]. \quad (5)$$

Here λ_{sf} stands for the electron-paramagnon interaction parameter, and ω_{sf} is the characteristic SF frequency (temperature).

The interplay between SFs and superconductivity is a well-known problem in the theory of superconductivity. In conventional superconductors, with electron-phonon pairing mechanism, FM SFs are known to compete with superconductivity, leading, e.g., to the lack of superconductivity in palladium.[22] More recently, SFs (paramagnons) were studied in the context of superconductivity in $MgCNi_3$,[10] or for elemental metals under pressure: Fe (Refs. 23 and 24) and Sc.[25] In fact, one finds that in case of SF superconductor the McMillan formula[8,9] may still be used, but the parameters λ and $\mu^\star$, applied when $\lambda_{sf}=0$ in Eq. (3), are then renormalized to[26] $\lambda_{eff}=\lambda_{ph}/(1+\lambda_{sf})$, $\mu^\star_{eff}=(\mu^\star+\lambda_{sf})/(1+\lambda_{sf})$.

First we calculate T_c without taking into account the SFs, i.e., using Eq. (3) with $\lambda_{eff}=\lambda_{ph}$ and $\mu^\star_{eff}=\mu^\star$. Since the value of Coulomb pseudopotential parameter $\mu^\star$ is unknown, we present T_c in a realistic range of $0.08<\mu^\star<0.18$ in Fig. 3. For the typical values of $\mu^\star$ and the calculated $\omega_{ph}=143$ K, we get $T_c=2.4$ K ($\mu^\star=0.10$) and 1.6 K ($\mu^\star=0.13$). Note, that when the prefactor in the McMillan equation is set to the original value[8] $\Theta/1.45$, and the experimental value[3] of Debye temperature $\Theta=310$ K is used, the resulting temperatures are higher: $T_c=4.0$ K ($\mu^\star=0.10$), 2.6 K ($\mu^\star=0.13$), 1.8 K ($\mu^\star=0.15$). These results demonstrate that depending on the prefactor, the experimental critical temperature $T_c=2.2$ K may be explained using the EPC constant $\lambda_{ph}=0.54$ derived within the rigid MT approximation, and taking $\mu^\star$ between 0.10 and 0.13.

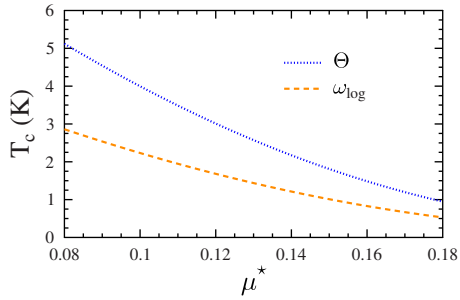

FIG. 3. (Color online) Critical temperature T_c as a function of Coulomb parameter $\mu^\star$ for $\lambda_{sf}=0$ and two prefactors in Eq. (3): $\omega_{ph}/1.20$ and $\Theta/1.45$. Parameters: $\lambda_{ph}=0.54$, $\lambda_{sf}=0$, $\omega_{ph}=143$ K, $\Theta=310$ K.

Next we analyze the possible influence of SFs on the transition temperature T_c. The electron-paramagnon mass enhancement λ_{sf} is treated as a parameter. It is important to note that if one explicitly takes into account the SF effect on the superconductivity, the starting value of $\mu^\star$ (i.e., before its renormalization by λ_{sf}) can be taken smaller than typically used (e.g., for Nb $\mu^\star=0.086$ was used in Ref. 26). Since Eq. (4) involves additional parameter, i.e., the characteristic paramagnon frequency ω_{sf}, in this case we plotted T_c against ω_{sf} for some representative values of λ_{sf} in Fig. 4. For $\omega_{sf}>100$ K the value of T_c is practically nonsensitive to the chosen ω_{sf}; thus this value was used in the calculations. Using Eq. (4), one finds that temperatures close to the observed $T_c=2.2$ K may be obtained for $\lambda_{sf}=0.03$ and $\mu^\star=0.08-0.09$ (corresponding to the effective $\mu^\star_{eff}=0.11-0.12$), i.e., $T_c=2.3$ K and $T_c=2.0$ K, respectively. Figure 4 shows that T_c quickly tends below 2 K when the electron-paramagnon interaction parameter $\lambda_{sf}\geq 0.05$.[27] Thus we conclude that the observed magnitude of the superconducting critical temperature can be explained taking into account the SF effects, but the λ_{sf} parameter has to be relatively small, $\lambda_{sf}\simeq 0.03$, if the EPC parameter $\lambda_{ph}=0.54$ obtained in our study is used.

Another interesting question concerns the influence of the spin gap, detected below $T^*=50$ K, on the superconducting

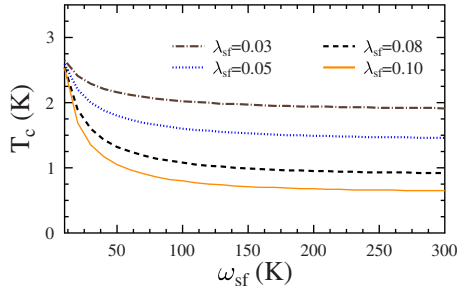

FIG. 4. (Color online) Critical temperature T_c as obtained from Eq. (4) for increasing paramagnon frequency ω_{sf} and for different values of λ_{sf}. Parameters: $\lambda_{ph}=0.54$, $\mu^\star=0.09$, $\omega_{ph}=143$ K.

state of Mo_3Sb_7. In view of the present results, this effect cannot be very strong, since (i) not all the Mo atoms are involved in building the singlet dimers (responsible for the gap[6]), and (ii) the Mo sublattice contribution to the total EPC constant λ_{ph} is about 35%, with the rest provided by the two Sb sublattices.

In summary, the results of electronic structure and phonon calculations were used to calculate the λ_{ph} parameter for the spin-fluctuation/spin-gap superconductor Mo_3Sb_7, within the rigid MT approximation. The estimated value of $\lambda_{ph}=0.54$ qualifies Mo_3Sb_7 as a medium-coupling superconductor. The experimentally observed critical temperature $T_c \simeq 2.2$ K may be correctly reproduced even including the presence of paramagnons, with small $\lambda_{sf} \simeq 0.03$. Thus, the spin fluctuations may exist in Mo_3Sb_7, but the electron-paramagnon interaction has to be moderate. Since the Mo contribution to the constant λ_{ph} is estimated to be comparable to Sb(1) and Sb(2) sublattices, the possible influence of spin gap on the superconductivity is expected to be rather weak. However, in the range of the EPC constant $\lambda_{ph} \sim 0.5$ the value of T_c is quite sensitive even to small changes in λ_{ph}, so a more quantitative explanation of the superconductivity in Mo_3Sb_7 requires further study.

This work was partly supported by the Polish Ministry of Science and Education under Projects No. 44/N-COST/2007/0 and No. N202 1975 33. A.M.O acknowledges support by the Foundation for Polish Science (FNP).

*Corresponding author: bartekw@fatcat.ftj.agh.edu.pl

[1] Z. Bukowski, D. Badurski, J. Stepien-Damm, and R. Troć, Solid State Commun. **123**, 283 (2002).
[2] V. M. Dmitriev, L. F. Rybaltchenko, L. A. Ishchenko, E. V. Khristenko, Z. Bukowski, and R. Troć, Supercond. Sci. Technol. **19**, 573 (2006).
[3] C. Candolfi, B. Lenoir, A. Dauscher, C. Bellouard, J. Hejtmanek, E. Santava, and J. Tobola, Phys. Rev. Lett. **99**, 037006 (2007).
[4] V. H. Tran, W. Miiller, and Z. Bukowski, arXiv:0803.2948 (unpublished).
[5] C. Candolfi, B. Lenoir, A. Dauscher, J. Hejtmanek, E. Santava, and J. Tobola, Phys. Rev. B **77**, 092509 (2008).
[6] V. H. Tran, W. Miiller, and Z. Bukowski, Phys. Rev. Lett. **100**, 137004 (2008).
[7] P. Piekarz, K. Parlinski, P. T. Jochym, A. M. Oleś, J. P. Sanchez, and J. Rebizant, Phys. Rev. B **72**, 014521 (2005).
[8] W. L. McMillan, Phys. Rev. **167**, 331 (1968).
[9] P. B. Allen and R. C. Dynes, Phys. Rev. B **12**, 905 (1975).
[10] O. V. Dolgov, I. I. Mazin, A. A. Golubov, S. Y. Savrasov, and E. G. Maksimov, Phys. Rev. Lett. **95**, 257003 (2005).
[11] A. Bansil, S. Kaprzyk, P. E. Mijnarends, and J. Tobola, Phys. Rev. B **60**, 13396 (1999).
[12] U. von Barth and L. Hedin, J. Phys.: Condens. Matter **5**, 1629 (1972).
[13] C. Candlofi (private communication).
[14] K. Parlinski, Z-. Q. Li, and Y. Kawazoe, Phys. Rev. Lett. **78**, 4063 (1997); K. Parlinski, Computer code PHONON, Cracow, 2008.
[15] G. Kresse and J. Furthmüller, Comput. Mater. Sci. **6**, 15 (1996); Phys. Rev. B **54**, 11169 (1996).
[16] J. P. Perdew, K. Burke, and M. Ernzerhof, Phys. Rev. Lett. **77**, 3865 (1996).
[17] The position of E_F close to such a sharp peak makes the $N(E_F)$ value sensitive to the computational details. In present calculations, using spherical potential approximation, gave $N(E_F) \simeq 165$ Ry^{-1}, whereas our full potential KKR calculations resulted in $N(E_F) \simeq 141$ Ry^{-1}.
[18] J. J. Hopfield, Phys. Rev. **186**, 443 (1969).
[19] G. D. Gaspari and B. L. Györffy, Phys. Rev. Lett. **28**, 801 (1972); I. R. Gomersall and B. L. Györffy, J. Phys. F: Met. Phys. **4**, 1204 (1974).
[20] W. E. Pickett, Phys. Rev. B **25**, 745 (1982).
[21] B. Wiendlocha, J. Tobola, and S. Kaprzyk, Phys. Rev. B **73**, 134522 (2006).
[22] N. F. Berk and J. R. Schrieffer, Phys. Rev. Lett. **17**, 433 (1966).
[23] I. I. Mazin, D. A. Papaconstantopoulos, and M. J. Mehl, Phys. Rev. B **65**, 100511(R) (2002).
[24] T. Jarlborg, Phys. Lett. A **300**, 518 (2002).
[25] S. K. Bose, J. Phys.: Condens. Matter **20**, 045209 (2008).
[26] J. M. Daams, B. Mitrović, and J. P. Carbotte, Phys. Rev. Lett. **46**, 65 (1981).
[27] If we use instead renormalized Eq. (3) we get $T_c=2.0$ K for $\mu^*_{eff}=0.11$ and $T_c=1.7$ K for $\mu^*_{eff}=0.12$, respectively.